

High energy density and high intensity physics

Measuring the orbital angular momentum of high-power laser pulses

R. Aboushelbaya, A.F. Savin, M. Mayr, B. Spiers, R. Wang (Clarendon Laboratory, University of Oxford, UK)
K. Glize, N. Bourgeois, R. Bingham (Central Laser Facility, STFC Rutherford Appleton Laboratory, Harwell Campus, Didcot, UK)

C. Spindloe (Scitech Precision Ltd, STFC Rutherford Appleton Laboratory, Didcot, UK)
P. Norreys (Clarendon Laboratory, University of Oxford, UK; Central Laser Facility, STFC Rutherford Appleton Laboratory, Harwell Campus, Didcot, UK; John Adams Institute for Accelerator Science, University of Oxford, UK)

In this article, we showcase the experimental results of methods to produce and characterise orbital angular momentum (OAM) carrying high-power lasers. The OAM pulses were produced on the Gemini laser of the Central Laser Facility using a continuous spiral phase plate.

Three different characterisation methods were then used to measure the OAM content of the beam. The methods that were used were a cylindrical lens diagnostic, an interferometric diagnostic, and a projective diagnostic. We further discuss the relative advantages and disadvantages of each method in the context of high-power laser experiments.

Reprinted with permission from R. Aboushelbaya, K. Glize, A.F. Savin et al. Measuring the orbital angular momentum of high-power laser pulses, *Phys. Plasmas* 27, 053107 (2020); doi: 10.1063/5.0005140

Contact: R. Aboushelbaya
 (ramy.aboushelbaya@physics.ox.ac.uk)

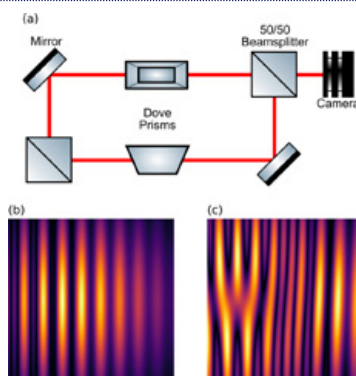


Figure 1: (a) Basic schematic showing the optical setup for the OAM interferometer. (b) and (c) Simulated results for the output of the interferometer in the case of a normal Gaussian profile and a LG with $l = 1$, respectively.

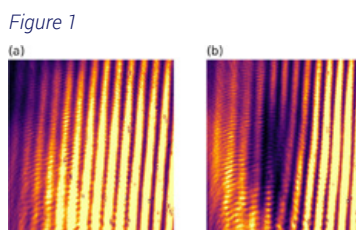


Figure 1

Figure 2

Figure 2: Experimental results for the interferometric diagnostic on the Gemini laser. (a) The result for the standard beam without the SPP, so $l = 0$, shows the typical fringes usually seen in interferometers. (b) When the SPP is placed in the beam path, the profile of the fringes changes and a discontinuity similar to the one in Figure 1 (c) is seen, indicating the presence of OAM

Application of compact laser-driven accelerator X-ray sources for industrial imaging

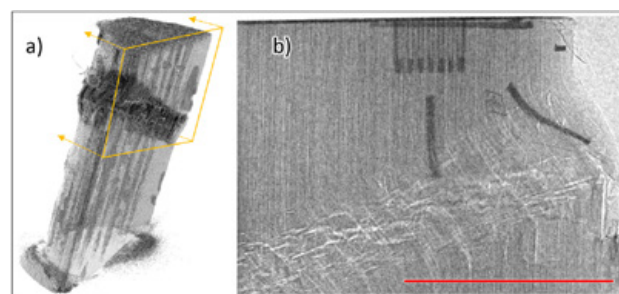
J.-N. Gruse, S.P.D. Mangles, Z. Najmudin, J.C. Wood (The John Adams Institute for Accelerator Science, Imperial College London, UK)
M.J.V. Streeter (The John Adams Institute for Accelerator Science, Imperial College London, UK; Physics Department, Lancaster University, UK)
C. Thornton, C.D. Armstrong, N. Bourgeois, C.D. Gregory, Y. Katzir, D. Neely, P.P. Rajeev, D.R. Rusby, C.M. Brenner, D.R. Symes (Central Laser Facility, STFC Rutherford Appleton Laboratory, Harwell Campus, Didcot, UK)
C.D. Baird (York Plasma Institute, Department of Physics, University of York, UK; Central Laser Facility, STFC Rutherford Appleton Laboratory, Harwell Campus, Didcot, UK)
S. Cipiccia (Diamond Light Source, Harwell Science and Innovation Campus, Didcot, UK)

O.J. Finlay (Physics Department, Lancaster University, UK)
N.C. Lopes (The John Adams Institute for Accelerator Science, Imperial College London, UK; GoLP, IPFN, Instituto Superior Tecnico, U. Lisboa, Portugal)
L.R. Pickard (National Composites Centre, Bristol and Bath Science Park, Bristol, UK)
K.D. Potter (Advanced Composites Collaboration for Science and Innovation (ACCIS) University of Bristol, UK)
C.I.D. Underwood, C.D. Murphy (York Plasma Institute, Department of Physics, University of York, UK)
J.M. Warnett, M.A. Williams (WMG, University of Warwick, UK)

X-rays generated by betatron oscillations of electrons in a laser-driven plasma accelerator were characterised and applied to imaging industrial samples. With a 125 TW laser, a low divergence beam with $5.2 \pm 1.7 \times 10^7$ photons mrad^{-2} per pulse was produced with a synchrotron spectrum with a critical energy of 14.6 ± 1.3 keV. Radiographs were obtained of a metrology test sample, battery electrodes, and a damage site in a composite material. These results demonstrate the suitability of the source for non-destructive evaluation applications. The potential for industrial implementation of plasma accelerators is discussed.

Reprinted from J.-N. Gruse et al. Application of compact laser-driven accelerator x-ray sources for industrial imaging, *Nucl. Instrum. Methods Phys. Res. Sect. A* 983, 164369 (2020), under the terms of the Creative Commons CC-BY license. doi: 10.1016/j.nima.2020.164369

Contacts: J.-N. Gruse (j.gruse16@imperial.ac.uk)
 D.R. Symes (dan.symes@stfc.ac.uk)



Kink band failure in a composite cylinder initiated by impact and propagated by compressive end loading. (a) tomographic reconstruction obtained using conventional lab x-ray CT (b) radiograph obtained with the laser-betatron source with carbon fibre tows visible. The red line indicates 1 cm. (For interpretation of the references to colour in this figure legend, the reader is referred to the web version of this article.)

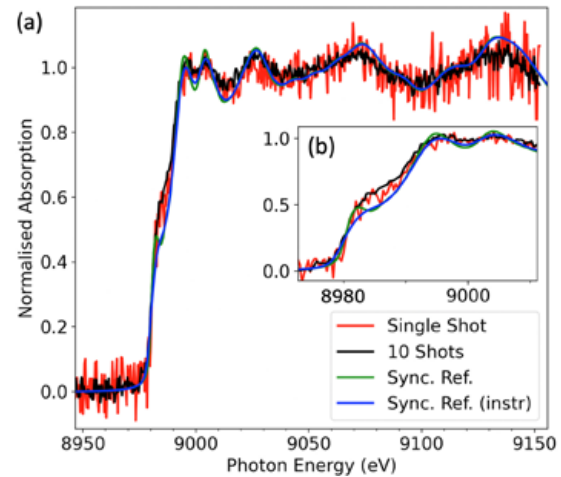
A laser-plasma platform for ultra-fast absorption spectroscopy: measuring the electron-ion equilibration rate of warm dense matter

B. Kettle, C. Colgan, E. Los, E. Gerstmayr, R.A. Baggott, R. Watt, S.J. Rose, S.P.D. Mangles (The John Adams Institute for Accelerator Science, Blackett Laboratory, Imperial College London, UK)
M.J.V. Streeter, N. Cavanagh, D. Riley, G. Sarri (Department of Physics and Astronomy, Queen's University Belfast, UK)
F. Albert (Lawrence Livermore National Laboratory, Livermore, California, USA)

S. Astbury, P.P. Rajeev, C. Spindloe, D. Symes, C. Thornton (Central Laser Facility, STFC Rutherford Appleton Laboratory, Harwell Campus, Didcot, UK)
K. Falk, M. Smid (Helmholtz-Zentrum Dresden-Rossendorf, Germany)
O. Lundh, K. Svendsen (Department of Physics, Lund University, Sweden)
A.G.R. Thomas (Center for Ultrafast Optical Science, University of Michigan, USA)

The K-edge absorption profile of a copper sample has been measured over a 200 eV spectral window on a single shot using the ultrafast x-rays from a laser-wakefield accelerator. This provides simultaneous snapshot details of the samples electronic and ionic configurations through the XANES (X-ray Absorption Near Edge Structure) and EXAFS (Extended X-ray Absorption Fine Structure) profiles. We discuss how, when combined with an appropriate sample heating technique, this unique x-ray source could be used to measure ultrafast processes in high density matter, for example the electron-ion equilibration rates of warm dense samples.

(a) Normalised absorption profile of a 4 μm copper foil. Data is shown for a single shot (red) and the average of ten shots (black). Both are compared to a synchrotron reference (green) and the same reference which has been convolved with our simulated instrument response (blue). (b) A zoomed view of the near edge profile.



Contact: B. Kettle (b.kettle@imperial.ac.uk)

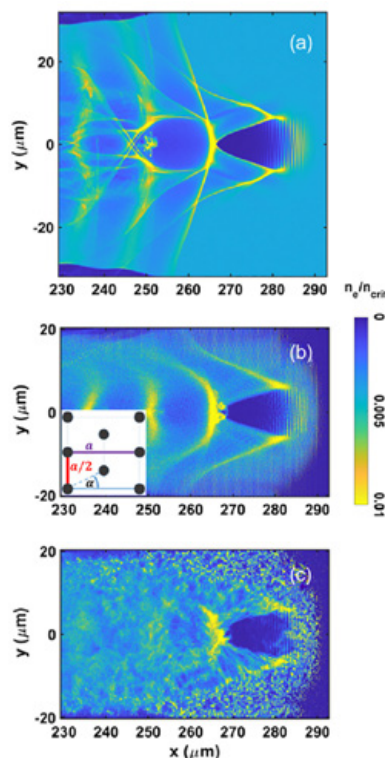
Nonlinear wakefields and electron injection in cluster plasma

M.W. Mayr, B. Spiers, R. Aboushelbaya, R.W. Paddock, C. Sillett, R.H.W. Wang (Clarendon Laboratory, University of Oxford, UK)
J.D. Sadler (Los Alamos National Laboratory, New Mexico, USA)
K. Krushelnick (Center for Ultrafast Optical Science, University of Michigan, USA)

P.A. Norreys (Central Laser Facility, STFC Rutherford Appleton Laboratory, Harwell Campus, Didcot, UK; Clarendon Laboratory, University of Oxford, UK; John Adams Institute for Accelerator Science and Department of Physics, University of Oxford, UK)

Laser and beam driven wakefields promise orders of magnitude increases in electric field gradients for particle accelerators for future applications. Key areas to explore include the emittance properties of the generated beams and overcoming the dephasing limit in the plasma. In this paper, the first in-depth study of the self-injection mechanism into wakefield structures from nonhomogeneous cluster plasmas is provided using high-resolution two dimensional particle-in-cell simulations. The clusters which are typical structures caused by ejection of gases from a high-pressure gas jet have a diameter much smaller than the laser wavelength. Conclusive evidence is provided for the underlying mechanism that leads to particle trapping, comparing uniform and cluster plasma cases. The accelerated electron beam properties are found to be tunable by changing the cluster parameters. The mechanism explains enhanced beam charge paired with large transverse momentum and energy which has implications for the betatron x-ray flux. Finally, the impact of clusters on the high-power laser propagation behavior is discussed.

Reprinted from M.W. Mayr et al. Nonlinear wakefields and electron injection in cluster plasma, *Rev. Accel. Beams* 23, 081303 (2020), under the terms of the Creative Commons Attribution 4.0 International License. doi: 10.1103/PhysRevAccelBeams.23.093501



Results of PIC simulations A, B, and C (parameters according to Table I in the published paper). Electron density normalized to critical density for (a) a uniform plasma, (b) a plasma of clusters arranged in a staggered grid, and (c) a plasma of clusters with random positions after 0.76 ps.

Contact: M.W. Mayr (manko.mayr@physics.ox.ac.uk)

Metre-scale conditioned hydrodynamic optical-field-ionized plasma channels

A. Picksley, A. Alejo, R.J. Shaloo, C. Arran, A. von Boetticher, J.A. Holloway, J. Jonnerby, O. Jakobsson, R. Walczak, S.M. Hooker (John Adams Institute for Accelerator Science and Department of Physics, University of Oxford, UK)

C. Thornton (Central Laser Facility, STFC Rutherford Appleton Laboratory, Harwell Campus, Didcot, UK)
 L. Corner (Cockcroft Institute for Accelerator Science and Technology, School of Engineering, University of Liverpool, UK)

We demonstrate through experiments and numerical simulations that low-density, low-loss, metre-scale plasma channels can be generated by employing a conditioning laser pulse to ionize the neutral gas collar surrounding a hydrodynamic optical-field-ionized (HOFI) plasma channel. We use particle-in-cell simulations to show that the leading edge of the conditioning pulse ionizes the neutral gas collar to generate a deep, low-loss plasma channel which guides the bulk of the conditioning pulse itself as well as any subsequently injected pulses. In proof-of-principle experiments, we generate conditioned HOFI (CHOFI) waveguides with axial electron densities of $n_{e0} \approx 1 \times 10^{17} \text{ cm}^{-3}$ and a matched spot size of $26 \mu\text{m}$. The power attenuation length of these CHOFI channels was calculated to be $L_{\text{att}} = (21 \pm 3) \text{ m}$, more than two orders of magnitude longer than achieved by HOFI channels. Hydrodynamic and particle-in-cell simulations demonstrate that metre-scale CHOFI waveguides with attenuation lengths exceeding 1 m could be generated with a total laser pulse energy of only 1.2 J per metre of channel. The properties of CHOFI channels are ideally suited to many applications in high-intensity light-matter interactions, including multi-GeV plasma accelerator stages operating at high pulse repetition rates.

Reprinted with permission from Picksley A, Alejo A, Shaloo RJ, et al., 2020, Meter-scale conditioned hydrodynamic optical-field-ionized plasma channels, *Phys. Rev. E* 102, 053201, ©2020 American Physical Society. doi: 10.1103/PhysRevE.102.053201

Contact: S.M. Hooker (simon.hooker@physics.ox.ac.uk)

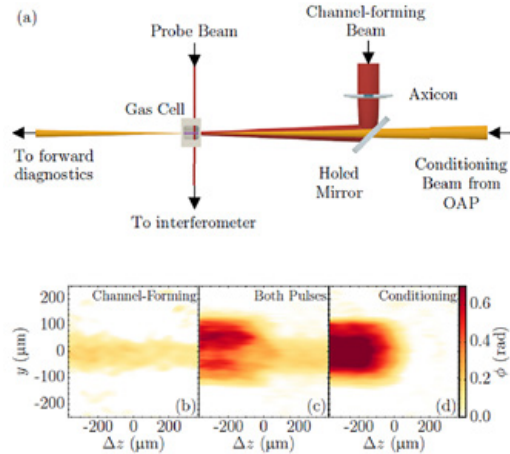


Figure 1: (a) Schematic of the experimental interaction region. [(b)–(d)] Phase shifts measured by the transverse probe beam at $z \approx 3.5 \text{ mm}$ for (b) the channel-forming pulse alone, (c) the channel-forming pulse and the conditioning pulse at a delay $\tau = 1.5 \text{ ns}$; and (d) the conditioning pulse alone

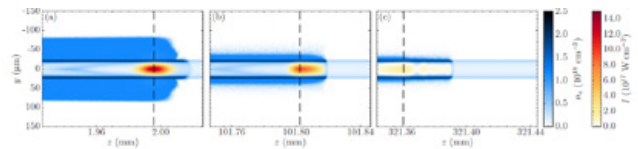


Figure 2: Transverse profiles of the electron density and the laser intensity when the peak of the conditioning pulse, indicated by the dashed line, has reached (a) $z = 2 \text{ mm}$, (b) $z = 101 \text{ mm}$, and (c) $z = 321 \text{ mm}$. The input intensity of the conditioning pulse was $I_{\text{peak}} = 6.0 \times 10^{17} \text{ W cm}^{-2}$

Guiding of high-intensity laser pulses in 100-mm-long hydrodynamic optical-field-ionized plasma channels

A. Picksley, A. Alejo, J. Cowley, J. Holloway, J. Jonnerby, A.J. Ross, R. Walczak, S.M. Hooker (John Adams Institute for Accelerator Science and Department of Physics, University of Oxford, UK)
 N. Bourgeois (Central Laser Facility, STFC Rutherford Appleton Laboratory, Harwell Campus, Didcot, UK)

L. Corner, H. Jones, L.R. Reid (Cockcroft Institute for Accelerator Science and Technology, School of Engineering, University of Liverpool, UK)
 L. Feder, H.M. Milchberg (Institute for Research in Electronics and Applied Physics, University of Maryland, USA)

Hydrodynamic optically-field-ionized (HOFI) plasma channels up to 100 mm long are investigated. Optical guiding is demonstrated of laser pulses with a peak input intensity of $6 \times 10^{17} \text{ W cm}^{-2}$ through 100 mm long plasma channels with on-axis densities measured interferometrically to be as low as $n_{e0} = (1.0 \pm 0.3) \times 10^{17} \text{ cm}^{-3}$. Guiding is also observed at lower axial densities, which are inferred from magneto-hydrodynamic simulations to be approximately $7 \times 10^{16} \text{ cm}^{-3}$. Measurements of the power attenuation lengths of the channels are shown to be in

good agreement with those calculated from the measured transverse electron density profiles. To our knowledge, the plasma channels investigated in this work are the longest, and have the lowest on-axis density, of any free-standing waveguide demonstrated to guide laser pulses with intensities above $>10^{17} \text{ W cm}^{-2}$.

Reprinted from Picksley A, Alejo A, Cowley J, et al., 2020, Guiding of high-intensity laser pulses in 100-mm-long hydrodynamic optical-field-ionized plasma channels, *Phys. Rev. Accel. Beams* 23, 081303, under the terms of the Creative Commons 4.0 International License. doi: 10.1103/PhysRevAccelBeams.23.081303

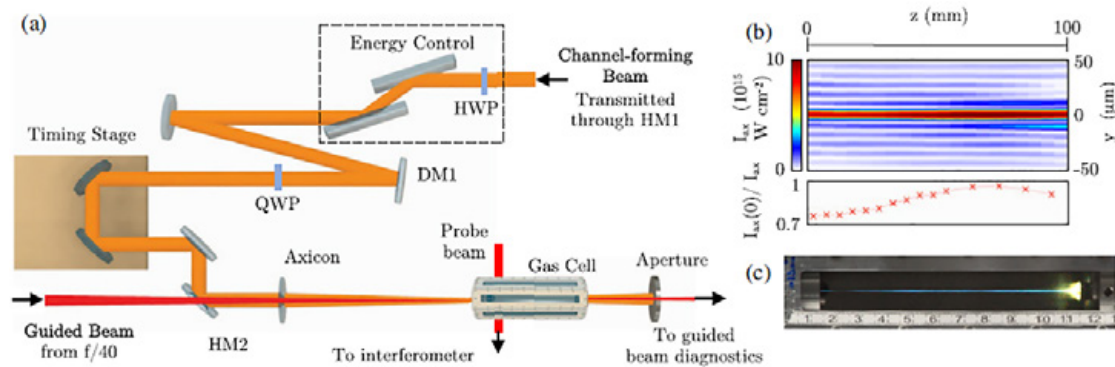


Figure 1: (a) Schematic diagram of the experiment layout. (b) Longitudinal variation of the transverse intensity profile of the axicon focus, measured in vacuo by a camera in the vacuum chamber. The red curve shows the axial intensity I_{ax} as a function of longitudinal position. (c) Time-integrated image of the visible plasma emission produced by the channel-forming beam focused into the gas cell at a fill pressure $P = 26 \text{ mbar}$. The scale visible at the bottom of the image is in cm. Note that the apparent decrease in plasma brightness near a scale reading of 2.5 cm arises from blackening of the cell window in that region, not from non-uniformity of the plasma.

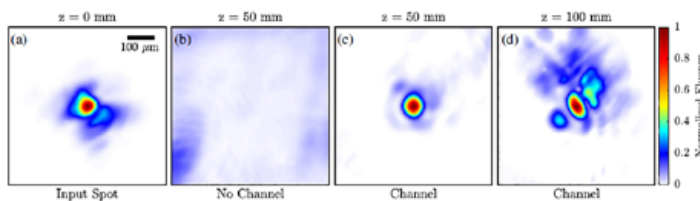


Figure 2: Measured transverse fluence profiles of the guided beam at: (a) focus, in vacuum; (b) $z = 50 \text{ mm}$, in vacuum; (c) $z = 50 \text{ mm}$, for $P = 68 \text{ mbar}$ and $\tau = 3.0 \text{ ns}$; (d) $z = 100 \text{ mm}$, for $P = 26 \text{ mbar}$ and $\tau = 2.7 \text{ ns}$. The transverse scale is the same for all plots, as indicated by the scale bar shown in (a). For plots (a), (c), and (d) the fluence is normalized to the peak value in that plot; the fluence scale for (b) is the same as in (a). Compared to (a), the fluence scales of (c) and (d) were increased by factors of approximately 4 and 7 respectively.

Contact: S.M. Hooker (simon.hooker@physics.ox.ac.uk)

Spectral and spatial characterisation of GeV-scale laser-driven positron beams

M.J.V. Streeter, N. Cavanagh, T. Audet, L. Calvin, G. Sarri (Centre for Plasma Physics, School of Mathematics and Physics, Queen's University Belfast, UK)
 C. Colgan, E. Los, B. Kettle, S.P.D. Mangles, Z. Najmudin (The John Adams Institute for Accelerator Science, Imperial College London, UK)

A. Antoine, M. Balcazar, J. Carderelli, Y. Ma, A.G.R. Thomas (Center for Ultrafast Optical Science, University of Michigan, USA)
 H. Ahmed, P.P. Rajeev, D.R. Symes (Central Laser Facility, STFC Rutherford Appleton Laboratory, Harwell Campus, Didcot, UK)

We report here on the first comprehensive characterisation of laser-driven positron beams with near-GeV energies, generated using Gemini. This work demonstrates that sizeable positron beams with micron-scale source size and nm-scale geometrical emittance can be generated

using laser parameters that are available with commercial systems. Such positron beams are of sufficient quality to be further injected in a plasma-based wakefield accelerator, demonstrating the first step towards a plasma-based positron accelerator.

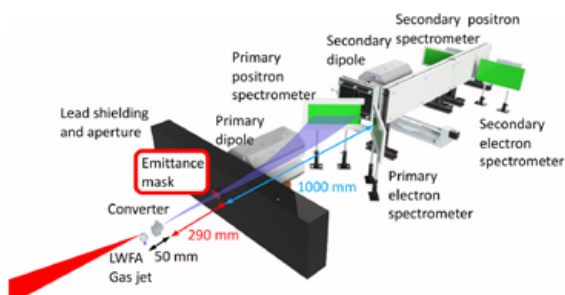


Figure 1: Schematic of the experimental setup. The laser is focused into the gas jet to drive the Laser-Wakefield Accelerator, which generates the primary electron beam. This electron beam produces electron-positron pairs in the converter which then propagate through an aperture in the lead wall. The primary dipole disperses the electron and positron beams (positrons shown in blue) onto the spectrometer screens. The emittance mask can be placed into the beam to measure the electron and positron beam spatial properties. A secondary electron spectrometer screen is used to improve the accuracy of the electron spectrum measurement. The secondary dipole and positron spectrometer screen is used to be perform energy selection.

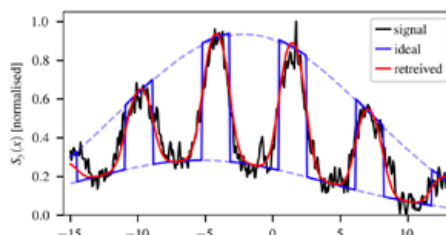


Figure 2: Example signal modulation fitting for beam parameters retrieval. The signal (black line) is taken for a central positron energy of 420MeV with a converter thickness of 8 mm. The retrieved signal (red line) corresponds to a source size of 127 μm . An ideal beam (zero source size) would produce a rectangular profile pattern (blue line) between the scattered signal and the beam amplitude (blue dashed lines).

Contact: G. Sarri (g.sarri@qub.ac.uk)

Automation and control of laser wakefield accelerators using Bayesian optimization

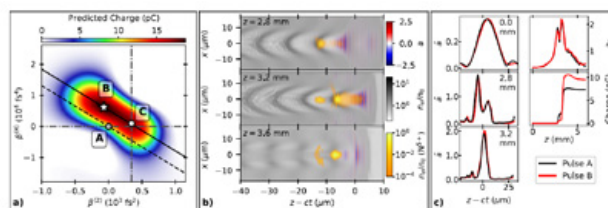
R.J. Shalloo, J.-N. Gruse, M. Backhouse, S.P.D. Mangles, Z. Najmudin, S. Rozario, M.J.V. Streeter (The John Adams Institute for Accelerator Science, Imperial College London, UK)
 S.J.D. Dann, N. Bourgeois, P.P. Rajeev, D.R. Symes, C. Thornton (Central Laser Facility, STFC Rutherford Appleton Laboratory, Harwell Campus, Didcot, UK)
 C.I.D. Underwood, C. Arran, C.D. Murphy, C.P. Ridgers, M.P. Selwood (York Plasma Institute, Department of Physics, University of York, UK)
 P. Hatfield (Clarendon Laboratory, University of Oxford, UK)

C.D. Baird (York Plasma Institute, Department of Physics, University of York, UK; Central Laser Facility, STFC Rutherford Appleton Laboratory, Harwell Campus, Didcot, UK)
 A.F. Antoine, M.D. Balcazar, J.A. Cardarelli, K. Krushelnick, A.G.R. Thomas (Center for Ultrafast Optical Science, University of Michigan, USA)
 J. Kang (Department of Chemical Engineering, University of Michigan, USA)
 N. Lu, A.J. Shahani (Department of Materials Science and Engineering, University of Michigan, USA)
 J. Osterhoff, K. Pöder (Deutsches Elektronen-Synchrotron DESY, Hamburg, Germany)

Laser wakefield accelerators promise to revolutionize many areas of accelerator science. However, one of the greatest challenges to their widespread adoption is the difficulty in control and optimization of the accelerator outputs due to coupling between input parameters and the dynamic evolution of the accelerating structure. Here, we use machine learning techniques to automate a 100 MeV-scale accelerator, which optimized its outputs by simultaneously varying up to six parameters including the spectral and spatial phase of the laser and the plasma density and length. Most notably, the model built by the algorithm enabled optimization of the laser evolution that might otherwise have been missed in single-variable scans. Subtle tuning of the laser pulse shape caused an 80% increase in electron beam charge, despite the pulse length changing by just 1%.

Shalloo, R.J., Dann, S.J.D., Gruse, J.N. et al. Automation and control of laser wakefield accelerators using Bayesian optimization. Nat Commun 11, 6355 (2020), under the terms of the Creative Commons 4.0 International License. doi: 10.1038/s41467-020-20245-6

Contact: R.J. Shalloo (r.shalloo@imperial.ac.uk)



Electron beam charge optimization through pulse shaping. **a** Surrogate model predicted charge on the $\beta^{(2)} - \beta^{(4)}$ plane at the optimal values of $\beta^{(3)}$ and **f**. Markers show the initial position projected onto this plane, A, and the optimal position, B. Marker C shows the likely end result of sequential 1D optimizations of $\beta^{(2)}$ and $\beta^{(4)}$ when starting from position A. The diagonal lines show the combination of $\beta^{(2)}$ and $\beta^{(4)}$ modifications that maintain an approximately constant pulse shape. **b** Snapshots from a PIC simulation showing the laser normalized vector potential **a**, the electron densities of the background plasma and the electrons released from the two inner ionization levels of nitrogen normalized to $n_0 = 1.2 \times 10^{19} \text{ cm}^{-3}$. **c** Left: axial laser field envelope at the given z positions and (right) maximum laser field, and total electron beam charge as functions of z position from simulations using the input laser pulse spectral phase coefficients from points A and B from **a**.

Electron trapping and reinjection in prepulse-shaped gas targets for laser-plasma accelerators

R.H.H. Scott, D.R. Symes, C. Hooker (Central Laser Facility, STFC Rutherford Appleton Laboratory, Harwell Campus, Didcot, UK)

C. Thornton, N. Bourgeois, J. Cowley, W. Ritterhofer, S.M. Hooker (Department of Physics and John Adams Institute for Accelerator Science, University of Oxford, UK)
T. Kleinwächter, J. Osterhoff (DESY, Hamburg, Germany)

A novel mechanism for injection, emittance selection, and postacceleration for laser wakefield electron acceleration is identified and described. It is shown that a laser prepulse can create an ionized plasma filament through multiphoton ionization and this heats the electrons and ions, driving an ellipsoidal blast-wave aligned with the laser-axis. The subsequent high-intensity laser-pulse generates a plasma wakefield which, on entering the leading edge of the blast-wave structure, encounters a sharp reduction in electron density, causing density down-ramp electron injection. The injected electrons are accelerated to ~ 2 MeV within the blast-wave. After the main laser-pulse has propagated past

the blast-wave, it drives a secondary wakefield within the homogenous background plasma. On exiting the blast-wave structure, the preaccelerated electrons encounter these secondary wakefields, are retrapped, and accelerated to higher energies. Due to the longitudinal extent of the blast-wave, only those electrons with small transverse velocity are retrapped, leading to the potential for the generation of electron bunches with reduced transverse size and emittance.

Reprinted from Scott RHH, Thornton C, Bourgeois N, et al. 2020 Phys. Rev. Accel. Beams 23, 111301, under the terms of the Creative Commons 4.0 International License doi: 10.1103/PhysRevAccelBeams.23.111301

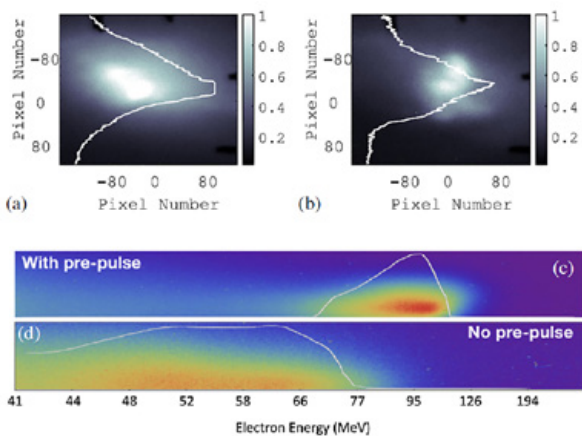
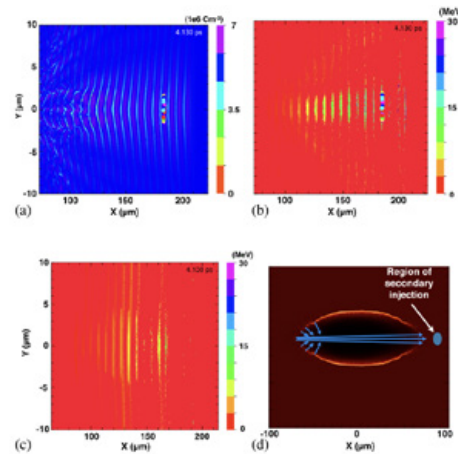


Figure 1: Electron beam energy deposition on a lanex screen, indicative of beam divergence (a) with prepulse, and (b) without. Note (a) is unfortunately saturated. Lines depict the relative signal and show both increased total signal (charge) and reduced divergence. Representative electron spectra with prepulse (c) and without (d). Spectra are imaged in the vertical direction corroborating (a) and (b).

Contact: R.H.H. Scott (robbie.scott@stfc.ac.uk)



Plasma parameters after the laser has propagated to $X = 205 \mu\text{m}$. The blast-wave ends at $X = 70 \mu\text{m}$. (a) The charge density distribution shows the wakefield structures created after the blast-wave; these wakes trap those electrons which are pre-accelerated within the blast-wave. (b) This plot of cell-averaged particle kinetic energy shows multiple bunches are accelerated to higher energies by the multiple wakes trailing the laser. The laser is not shown, but is centred at $X = 205 \mu\text{m}$. Only those electrons originating from the nitrogen atoms are shown. (c) As per (b) but with a density profile which only varies as a function of x . Here the lateral extent of the bunches is significantly increased from $\sim 2 \mu\text{m}$ to $10 \mu\text{m}$. (d) Blue arrows illustrate the initial propagation directions of those electrons injected at the blast-wave. The electrons are injected approximately perpendicularly to the blast-wave at a given location, so only those with small divergence (near $y = 0$) enter the region of secondary injection.

Development of control mechanisms for a laser wakefield accelerator-driven bremsstrahlung x-ray source for advanced radiographic imaging

C.I.D. Underwood, C.D. Murphy, M.P. Selwood (York Plasma Institute, Department of Physics, University of York, UK)

C.D. Baird (York Plasma Institute, Department of Physics, University of York, UK; Central Laser Facility, STFC Rutherford Appleton Laboratory, Harwell Campus, Didcot, UK)

C.D. Armstrong, C. Thornton, D. Rusby, D.R. Symes, C.M. Brenner (Central Laser Facility, STFC Rutherford Appleton Laboratory, Harwell Campus, Didcot, UK)

O.J. Finlay (The Cockcroft Institute, Keckwick Lane, Daresbury, UK)

M.J.V. Streeter, J-N. Gruse, Z. Najmudin (The John Adams Institute for Accelerator Science, Imperial College London, UK)

N. Brierley (The Manufacturing Technology Centre, Ansty Park, Coventry, UK)

S. Cipiccia (Diamond Light Source, Harwell Science and Innovation Campus, Didcot, UK)

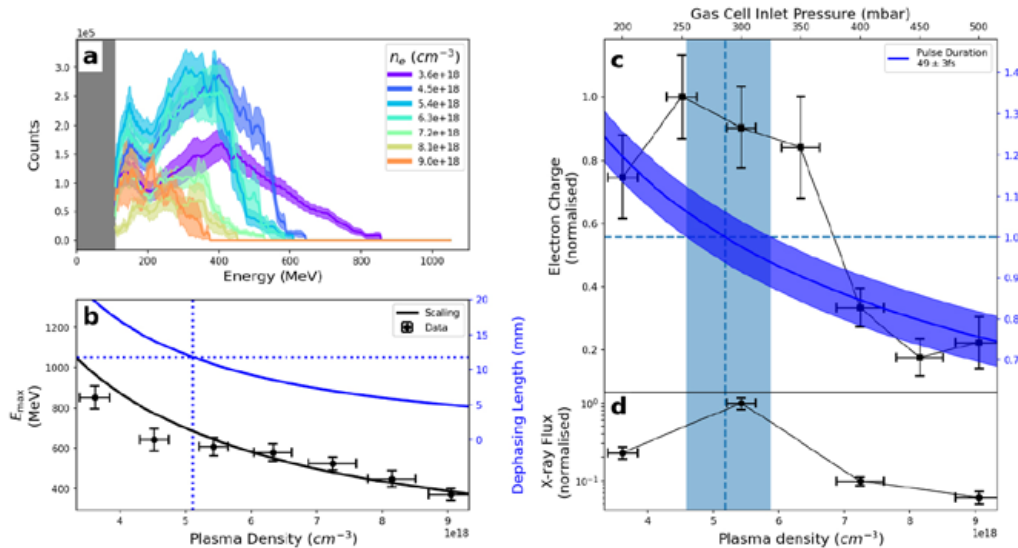
P. McKenna (SUPA Department of Physics, University of Strathclyde, Glasgow, UK)

D. Neely (Central Laser Facility, STFC Rutherford Appleton Laboratory, Harwell Campus, Didcot, UK; SUPA Department of Physics, University of Strathclyde, Glasgow, UK)

A high power laser was used to accelerate electrons in a laser-driven wakefield accelerator. The high energy electrons were then used to generate an x-ray beam by passing them through a converter target. This bremsstrahlung source was characterised and used to perform penetrative imaging of industrially relevant samples. The photon spectrum had a critical energy in excess of 100 MeV and a source size smaller than the resolution of the diagnostic ($\approx 150 \mu\text{m}$). Simulations

indicate a significantly smaller source is achievable. Variations in the x-ray source characteristics were realised through changes to the plasma and converter parameters while simulations confirm the adaptability of the source. Imaging of high areal density objects with $150 \mu\text{m}$ resolution was performed, demonstrating the unique advantages of this novel source.

Reprinted from C.I.D. Underwood et al 2020 Plasma Phys. Control. Fusion 62 124002, under the terms of the Creative Commons 4.0 International License. doi: 10.1088/1361-6587/abbebe



The measured source characteristics with respect to electron plasma density (n_e). (a) The average electron spectrum for the different plasma densities used. The shaded regions correspond to one standard error. (b) The maximum electron energy, showing that when the dephasing length (solid blue line) is shorter than the gas cell (dotted blue line) then the maximum energy follows the inverse scaling (solid black line). (c) Total electron charge (normalised) vs. n_e shown in black. The blue line represents $\lambda_p/c\tau$ for the measured pulse length of 49 ± 3 fs. The point where the pulse duration is matched to the plasma wavelength is shown (marked with the blue dashed line, and the shaded region the error in this value). (d) The x-ray flux (normalised) measured with the caesium iodide (CsI) array for the 1 mm iron converter target. The x-ray flux maximum corresponds to the electron beam with peak charge.

Contact: C.I.D. Underwood (christopher.underwood@york.ac.uk)

Self-Referencing Spectral Interferometric Probing of the Onset Time of Relativistic Transparency in Intense Laser-Foil Interactions

S.D.R. Williamson, R. Wilson, M. King, M. Duff, B. Gonzalez-Izquierdo, Z.E. Davidson, A. Higginson, R.J. Gray, P. McKenna (SUPA Department of Physics, University of Strathclyde, Glasgow, UK)

N. Booth, S. Hawkes (Central Laser Facility, STFC Rutherford Appleton Laboratory, Harwell Campus, Didcot, UK)

D. Neely (SUPA Department of Physics, University of Strathclyde, Glasgow, UK; Central Laser Facility, STFC Rutherford Appleton Laboratory, Harwell Campus, Didcot, UK)

Irradiation of an ultrathin foil target by a high-intensity laser pulse drives collective electron motion and the generation of strong electrostatic fields, resulting in ultrabright sources of high-order harmonics and energetic ions. The ion energies can be significantly enhanced if the foil undergoes relativistic self-induced transparency during the interaction, with the degree of enhancement depending in part on the onset time of transparency. We report on a simple and effective approach to diagnose the time during the interaction at which the foil becomes transparent to the laser light, providing a route to optically controlling and optimizing ion acceleration and radiation generation. The scheme involves a self-referencing

approach to spectral interferometry, in which coherent transition radiation produced at the foil rear interferes with laser light transmitted through the foil. The relative timing of the onset of transmission with respect to the transition-radiation generation is determined from spectral fringe spacing and compared to simultaneous frequency-resolved optical-gating measurements. The results are in excellent agreement, and are discussed with reference to particle-in-cell simulations of the interaction physics and an analytical model for the onset time of transparency in ultrathin foils.

Reprinted with permission from Williamson SDR, Wilson R, King M, et al., 2020, Self-Referencing Spectral Interferometric Probing of the Onset Time of Relativistic Transparency in Intense Laser-Foil Interactions, Phys. Rev. Applied 14, 034018, ©2020 American Physical Society. doi: 10.1103/PhysRevApplied.14.034018

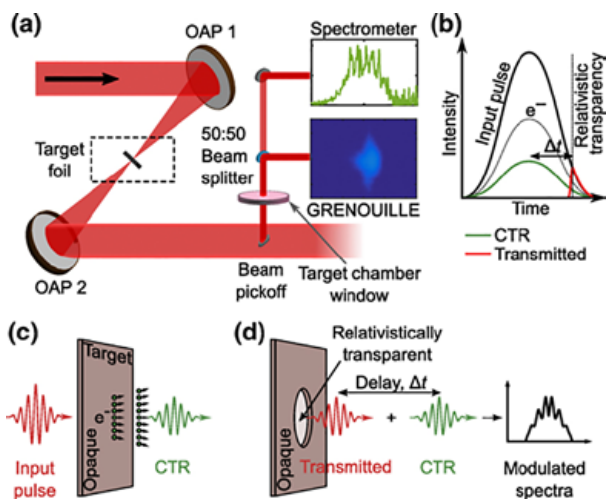


Figure 1: (a) Schematic of the experiment showing the laser-focusing geometry and diagnostic channel. The drive laser pulse is focused using off-axis parabola OAP 1 and the light collected at the target rear, using OAP 2, is directed for simultaneous measurement using a GRENOUILLE and an optical spectrometer. (b) Schematic illustrating the timing of the CTR generation and transmitted part of the laser pulse, where the temporal separation (Δt) relates to the onset time of RSIT relative to the peak of the laser pulse interacting and fast electron generation. (c,d) Schematic of the laser-plasma interaction before, (c), and after, (d), RSIT, resulting in a generated pulse of CTR light and the transmitted laser pulse, with a temporal delay defined by the onset time for RSIT.

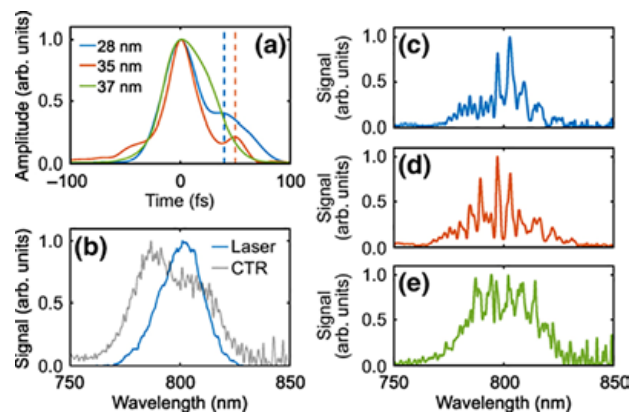


Figure 2: (a) Temporal-intensity profile extracted from GRENOUILLE measurements for three given target thicknesses, for fixed drive laser pulse duration $\tau_L = 40$ fs. (b) Representative measurements of the input laser spectrum and the generated CTR spectrum. (c)–(e) Spectral measurements for (c) $d = 28$ nm, (d) $d = 35$ nm, and (e) $d = 37$ nm targets.

Contact: P. McKenna (paul.mckenna@strath.ac.uk)

Influence of target-rear-side short scale length density gradients on laser-driven proton acceleration

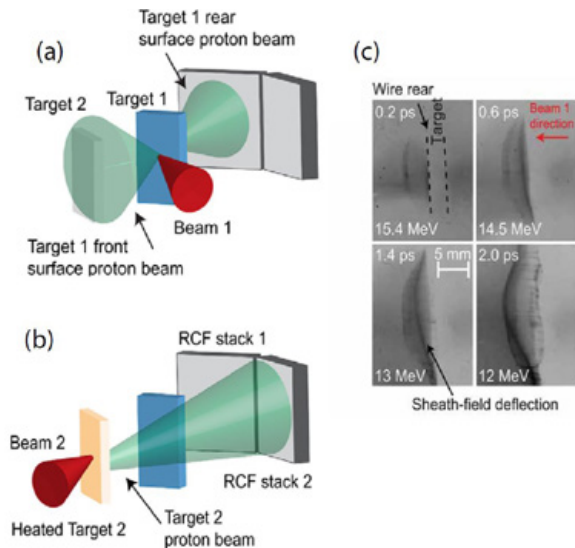
A. Higginson, R. Wilson, J. Goodman, R.J. Dance, N.M.H. Butler, R.-J. Gray (SUPA, Department of Physics, University of Strathclyde, Glasgow, UK)
M. King, P. McKenna (SUPA, Department of Physics, University of Strathclyde, Glasgow, UK; The Cockcroft Institute, Sci-Tech Daresbury, Warrington, UK)
C.D. Armstrong, D. Neely (SUPA, Department of Physics, University of Strathclyde, Glasgow, UK; Central Laser Facility, STFC Rutherford Appleton Laboratory, Harwell Campus, Didcot, UK)

M. Notley, D.C. Carroll (Central Laser Facility, STFC Rutherford Appleton Laboratory, Harwell Campus, Didcot, UK)
Y. Fang, X.H. Yuan (Key Laboratory for Laser Plasmas and CICIFSA, School of Physics and Astronomy, Shanghai Jiao Tong University, People's Republic of China)

In this article the influence of a short plasma density scale length on laser-driven proton acceleration, in the TNSA regime, is investigated experimentally by heating and driving the expansion of a large area on the target rear. Key parameters of the generated protons, such as maximum proton energy, proton flux and divergence, are all measured to decrease with increasing plasma expansion. Even for a small plasma scale length of the order of the laser wavelength ($\sim 1 \mu\text{m}$), a substantial decrease in the number of protons over a wide spectral range is measured. Through a combination of radiation-hydrodynamic and particle-in-cell simulations new insight into the underlying physics is observed, providing new understanding of the strong influence even a small plasma density gradient can have on laser-driven ion acceleration. The findings have implications for applications that require efficient laser energy conversion to ions, such as the proton-driven fast-ignition scheme of inertial confinement fusion (ICF).

Reproduced from A Higginson et al 2021 *Plasma Phys. Control. Fusion* 63 114001, under the terms of the Creative Commons Attribution 4.0 licence. doi: 10.1088/1361-6587/ac2035

Contact: P. McKenna (paul.mckenna@strath.ac.uk)



Schematic of the experimental set-up, showing the two steps corresponding to the dual beam interaction. (a) interaction between laser beam 1 and target 1, with the rear-surface-accelerated (TNSA) protons characterised using RCF 1 and the front-surface-accelerated protons irradiating and heating target 2. (b) Second interaction, between laser beam 2 and target 2, which occurs after a controlled temporal delay relative to the protons from the first interaction arriving at the rear of target 2. (c) Example RCF measurements of TNSA protons from target 2 probing the spatio-temporal evolution of the sheath-field on Target 1.

Narrow-band acceleration of gold ions from ultra-thin foils

P. Martin, F. Hanton, D. Gwynne, M. Borghesi, S. Kar (Centre for Plasma Physics, Queen's University Belfast, UK)

H. Ahmed, J. S. Green (Central Laser Facility, STFC Rutherford Appleton Laboratory, Harwell Campus, Didcot, UK)

D. Doria (ELI NP, Magurele, Romania)

A. Alejo (IGFAE, Universidade de Santiago de Compostela, Spain)

A. Macchi (Istituto Nazionale di Ottica, Consiglio Nazionale delle Ricerche (CNR/INO), Laboratorio Adriano Gozzini, Pisa, Italy)

M. Cerchez, M. Swantusch, O. Willi (Institut für Laser-und Plasmaphysik, Heinrich-Heine-Universität, Düsseldorf, Germany)

J. Fernandez-Tobias, J. A. Ruiz (Instituto de Fusion Nuclear, Universidad Politécnica de Madrid, Spain)

D. MacLellan, P. McKenna (Department of Physics, University of Strathclyde, UK)

S. Zhai (Shanghai Normal University, China)

In this paper we demonstrate, for the first time, the laser-driven acceleration of extremely heavy gold ions to a narrow-band spectral bunch. The Au ion energies are the highest reported to date, and the flux achieved exceeds other notable works by orders of magnitude. Simulations reveal an interplay of multiple acceleration mechanisms,

whereby the high flux Au bunch is generated from the influence of strong radiation pressure acceleration. We also demonstrate scalability of this phenomenon for multi-PW laser systems. Such high flux, energetic Au ion beams would be of profound interest for applications in laboratory astrophysics, and nuclear physics research.

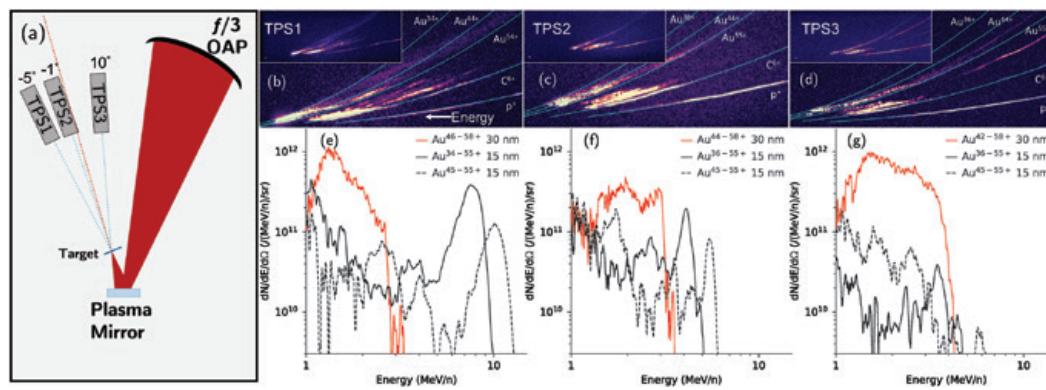


Figure 1

Figure 1: (a) Schematic of the experimental setup, TPS1–3 represents the three high resolution Thomson parabola spectrometers (TPS) deployed at different angles (as labelled) with respect to target normal (red dashed line). (b, c, d) Raw image plate data from each TPS on 15 nm gold foil, with example ion traces indicated in cyan, where ion energies increase going from right to left on each image. Au ion traces (as labelled) represent the bounds of the charge ranges over which spectra were integrated. The insets show the full IP image. (e, f, g) Au ion spectra, in order from TPS1 to TPS3, for 15 nm (black) and 30 nm (red) targets. For both thicknesses, spectra are shown representing signal integration over the entirety of the charge states observed (solid lines, charge ranges are as labelled in the legend), and energies calculated assuming a central charge of 44+ and 51+ for the 15 and 30 nm targets, respectively. Additionally, for the 15 nm target, a second spectrum was generated integrating signal only for charges above 45+ (dashed lines), representing most of the ion signal, at a central charge of 51+. The difference in ion energy at the spectral peak of solid and dashed black lines is due to the chosen charge states for energy calculation. The Au ion flux in the spectrum was calculated by using the absolute calibration of the detector (BAS-TR image plate) response to laser driven Au ions shown in doi: 10.1063/5.0079564.

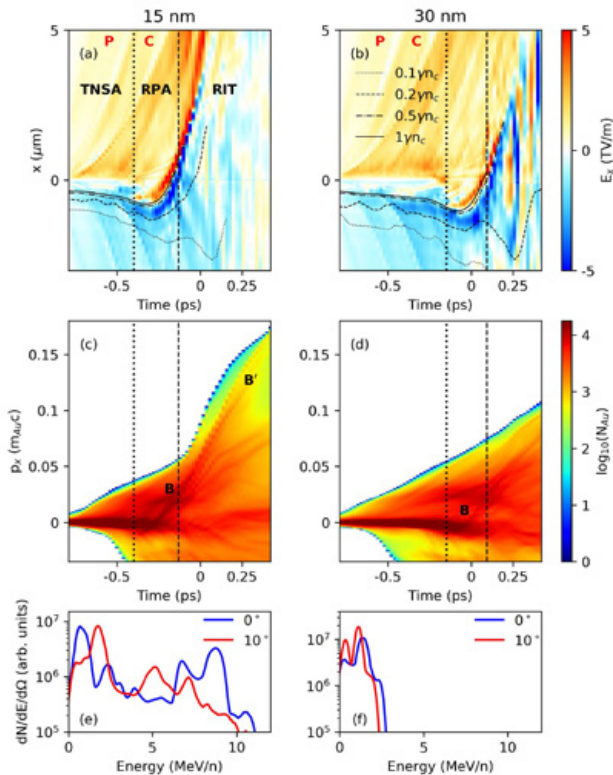


Figure 2

Figure 2: 2D PIC simulations comparing two target thicknesses, showing (a,b) the time evolution of the cycle averaged longitudinal electric field along the laser axis for 15 nm and 30 nm thick targets, respectively. The black curves indicate the positions of (relativistically corrected) electron density fronts at 0.1, 0.2, 0.5, and 1 times critical, while the vertical dotted and dashed lines indicate the transitions between each acceleration phase: TNSA, RPA, and RIT. (c,d) The time evolution of the Au ion momentum spectrum (integrated over all charge states, to account for ionisation during the pulse) along the laser axis, for each thickness. Time is measured relative to the incidence of the pulse peak at the initial target front surface ($x=0 \mu\text{m}$). Au^{40-51+} ion energy spectra from the 15 nm (e) and 30 nm (f) targets are shown, taken at $t = 270 \text{ fs}$, inside 1 degree half-angle cones directed on-axis (blue -0°) and off-axis (red -10°).

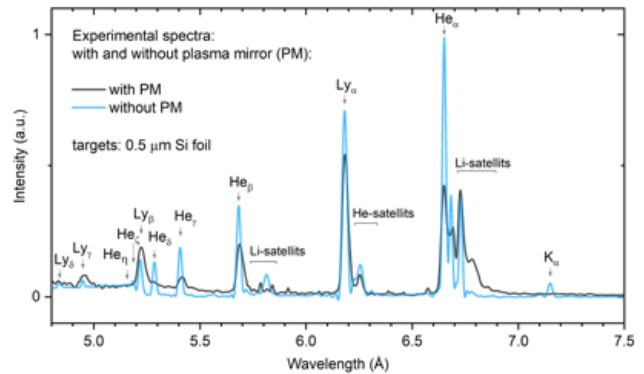
Contact: P. Martin (p.martin@qub.ac.uk)

Determining the short laser pulse contrast based on X-Ray emission spectroscopy

A.S. Martynenko (Joint Institute for High Temperatures of Russian Academy of Sciences, Moscow, Russia)
I.Yu. Skobelev, S.A. Pikuz, S.N. Ryazantsev (Joint Institute for High Temperatures of Russian Academy of Sciences, Moscow, Russia; National Research Nuclear University MEPhI, Moscow, Russia)
C. Baird, L. Doehl, P. Durey, D. Farley, K. Lancaster, C.D. Murphy, N. Woolsey (York Plasma Institute, Department of Physics, University of York, UK)

N. Booth, C. Spindloe (Central Laser Facility, STFC Rutherford Appleton Laboratory, Harwell Campus, Didcot, UK)
R. Kodama (Open and Transdisciplinary Research Initiative, Osaka University, Japan)
P. McKenna (Department of Physics, SUPA, University of Strathclyde, Glasgow, UK)
T.A. Pikuz (Joint Institute for High Temperatures of Russian Academy of Sciences, Moscow, Russia; Open and Transdisciplinary Research Initiative, Osaka University, Japan)

The interaction of high-power short lasers with solid density targets is an important application of modern solid state lasers. However, uncertainties in measurements due to lack of information on the laser pedestal-to-peak contrast limits the validity of many conclusions. We show that X-ray spectral measurements can provide a straightforward way for accessing the laser pedestal-to-peak contrast. The experiments use silicon targets and relativistic laser intensities of 3×10^{20} W/cm² with a pulse duration of 1 ps. By not using or using a plasma mirror we compare low and high contrast measurements of the Ly- α line and its satellites to show that these lines are an effective laser contrast diagnostic. This diagnostic has potential to reduce uncertainty in future laser-solid interaction studies.



Spectra of the picosecond laser plasma formed by laser pulses of different contrasts: a spectrum from a relatively high contrast is shown by the orange curve and compared to a spectrum from a relatively low contrast interaction by the black curve. The spectra allow an estimation of the plasma density at the time of arrival of a main laser beam.

Reproduced from the Accepted Version (<https://eprints.whiterose.ac.uk/170892/>) of Martynenko, A. S., Skobelev, I. Yu, Pikuz, S. A. et al. (13 more authors) (2021) Determining the short laser pulse contrast based on X-Ray emission spectroscopy. HIGH ENERGY DENSITY PHYSICS. 100924. ISSN 1574-1818 under the terms of the Creative Commons licence CC-BY-NC-ND 2.5. A definitive version was subsequently published in High Energy Density Physics, 38:100924 (2021) © 2021, Elsevier. doi: 10.1016/j.hedp.2021.100924

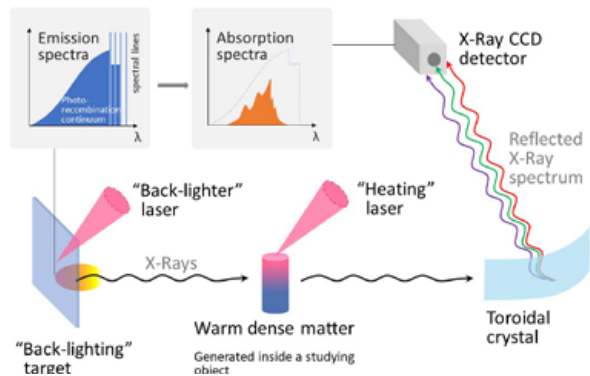
Contact: S.A. Pikuz (spikuz@gmail.com)

Optimization of a laser plasma-based x-ray source according to WDM absorption spectroscopy requirements

A.S. Martynenko (Joint Institute for High Temperatures of Russian Academy of Sciences, Moscow, Russia)
S.A. Pikuz, I.Yu. Skobelev, S.N. Ryazantsev (Joint Institute for High Temperatures of Russian Academy of Sciences, Moscow, Russia; National Research Nuclear University MEPhI, Moscow, Russia)
C. Baird, L. Döhl, P. Durey, D. Farley, K. Lancaster, C. D. Murphy, N. Woolsey (York Plasma Institute, Department of Physics, University of York, UK)

N. Booth, C. Spindloe (Central Laser Facility, STFC Rutherford Appleton Laboratory, Harwell Campus, Didcot, UK)
R. Kodama (Open and Transdisciplinary Research Initiative, Osaka University, Japan; Institute of Laser Engineering, Osaka University, Japan)
P. McKenna (Department of Physics, SUPA, University of Strathclyde, Glasgow, UK)
T.A. Pikuz, A.Ya. Faenov (Joint Institute for High Temperatures of Russian Academy of Sciences, Moscow, Russia; Open and Transdisciplinary Research Initiative, Osaka University, Japan)

X-ray absorption spectroscopy is a recognised diagnostic technique for experimental studies of warm dense matter. It requires a short-lived X-ray source with a sufficiently high emissivity and without characteristic lines in a spectral range of interest. In the present work, we discuss the choice of the optimal material and thickness to obtain a bright source in the wavelength range of 2 - 6 Å (~2 - 6 keV) considering relatively low Z elements. We demonstrate that the highest emissivity of solid aluminium and silicon foil targets irradiated with a high-contrast sub-kJ laser pulse of 1 ps is obtained when the thickness of the target is close to 10 μm. An outer plastic layer can further increase the emissivity.



Reproduced from Matter Radiat. Extremes 6, 014405 (2021), under the terms of a Creative Commons Attribution (CC BY) license. doi: 10.1063/5.0025646

Principle scheme of absorption spectroscopy with a laser-based X-ray source. The focus is on the photorecombination continuum emission from solid-density plasmas to produce a featureless spectral continuum of high intensity that can be used e.g. for X-ray absorption spectroscopy studies of warm dense matter.

Contacts: A.S. Martynenko (artmarty@mail.ru)
 S.A. Pikuz (spikuz@gmail.com)

Effect of plastic coating on the density of plasma formed in Si foil targets irradiated by ultra-high-contrast relativistic laser pulses

A.S. Martynenko, S.A. Pikuz, I.Yu. Skobelev, S.N. Ryazantsev (Joint Institute for High Temperatures of Russian Academy of Sciences, Moscow, Russia; National Research Nuclear University MEPhI, Moscow, Russia)

C. Baird, L. Doehl, P. Durey, D. Farley, K. Lancaster, C.D. Murphy, N. Woolsey (York Plasma Institute, Department of Physics, University of York, UK)

N. Booth, C. Spindloe (Central Laser Facility, STFC Rutherford Appleton Laboratory, Harwell Campus, Didcot, UK)

R. Kodama (Open and Transdisciplinary Research Initiative, Osaka University, Japan; Institute of Laser Engineering, Osaka University, Japan)

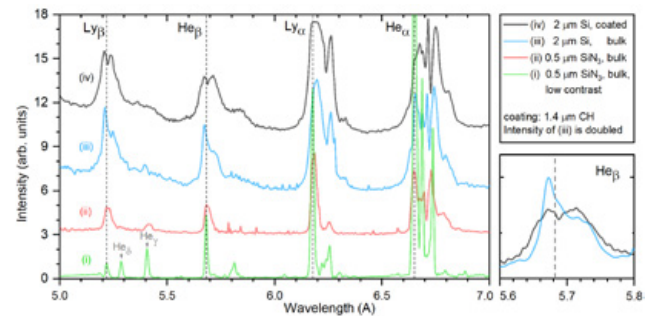
P. McKenna (Department of Physics, SUPA, University of Strathclyde, Glasgow, UK)

T.A. Pikuz, A.Ya. Faenov (Joint Institute for High Temperatures of Russian Academy of Sciences, Moscow, Russia; Open and Transdisciplinary Research Initiative, Osaka University, Japan)

The formation of matter with high energy density occurs in inertial fusion and in astrophysical and geophysical systems. In this context, it is important to couple as much energy as possible into a target while maintaining a high density. A recent experimental campaign using buried layer (or "sandwich" type) targets and the Vulcan PW ultra-high laser contrast resulted in 500 Mbar pressures in near-solid density plasmas (corresponding to an energy density of about 4.6×10^7 J/cm³). The densities and temperatures of the generated plasma were measured by analysing the X-ray spectral line profiles and relative intensities.

Reprinted with permission from A Martynenko et al. Effect of plastic coating on the density of plasma formed in Si foil targets irradiated by ultra-high-contrast relativistic laser pulses, *Phys. Rev. E* 101, 043208, © American Physical Society 2020. doi: 10.1103/PhysRevE.101.043208

Contact: S.A. Pikuz (spikuz@gmail.com)



Experimental X-ray spectra obtained by laser pulse irradiation of (i) 0.5 μm SiN₃ uncoated film without plasma mirror, (ii) 0.5 μm SiN₃ uncoated film with plasma mirror, (iii) 2 μm Si film coated on both sides with 1.4 μm CH plastic layers, and (iv) 2 μm Si uncoated film. The intensity of curve (i) is divided by a factor of 2 and the intensity of curve (iii) is doubled. One can see an influence of the plastic coating and the plasma mirror on the plasma density.

Influence of spatial-intensity contrast in ultraintense laser-plasma interactions

R. Wilson, N.M.H. Butler, T.P. Frazer, M.J. Duff, A. Higginson, R.J. Dance, J. Jarrett, Z.E. Davidson, R.J. Gray (SUPA Department of Physics, University of Strathclyde, Glasgow, UK)

M. King, P. McKenna (SUPA Department of Physics, University of Strathclyde, Glasgow, UK;

The Cockcroft Institute, Sci-Tech Daresbury, Warrington, UK)

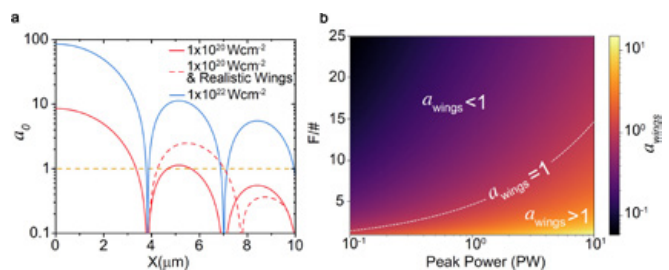
D.C. Carroll, S.J. Hawkes, R.J. Clarke (Central Laser Facility, STFC Rutherford Appleton Laboratory, Harwell Campus, Didcot, UK)

C.D. Armstrong, D. Neely (SUPA Department of Physics, University of Strathclyde, Glasgow, UK; Central Laser Facility, STFC Rutherford Appleton Laboratory, Harwell Campus, Didcot, UK)

H. Liu (Central Laser Facility, STFC Rutherford Appleton Laboratory, Harwell Campus, Didcot, UK; Beijing National Laboratory for Condensed Matter Physics, Institute of Physics, Chinese Academy of Sciences, Beijing, China)

There has been continual drive to increase the achievable peak intensity of laser light, resulting in an average increase of two to three orders of magnitude per decade. Further increase is achievable via tighter focusing, however the influence the focal spot spatial profile plays is not fully understood. In this article it is demonstrated that the spatial-intensity distribution, specifically the ratio of the intensity in the peak of the spot to the surrounding halo of light, is important in the interaction of ultraintense laser pulses with solid targets. Through the comparison of TNSA proton acceleration from targets irradiated by a near-diffraction-limited wavelength scale focal spot and larger F-number focusing, we find that the focal spot spatial-intensity contrast strongly influences laser energy coupling to fast electrons. From this study it is clear that for future multi-petawatt laser systems, spatial-intensity contrast is potentially as important as temporal-intensity contrast.

Reproduced from Wilson, R., King, M., Butler, N.M.H. et al. Influence of spatial-intensity contrast in ultraintense laser-plasma interactions. *Sci Rep* 12, 1910 (2022), under the terms of the Creative Commons Attribution 4.0 International License. doi: 10.1038/s41598-022-05655-4



(a) Normalised vector potential (a_0) as a function of spot radius, for idealised (Airy disk) focal spots at two given peak intensities, each of the same diameter. The dashed red data illustrates a case for which the intensity distribution is non-ideal, resulting in a higher intensity in the wings (a degradation of the spatial-intensity contrast). The dashed orange line marks the relativistic threshold intensity for 1 μm light. (b) Normalised vector potential of the laser light in the focal spot wings, a_{wings} , as a function of laser pulse power and focusing geometry. The $a_{wings} = 1$ curve marks the threshold for which the intensity in the wings is relativistic.

Contact: P. McKenna (paul.mckenna@strath.ac.uk)